Supplement of The Cryosphere, 20, 1815–1840, 2026
https://doi.org/10.5194/tc-20-1815-2026-supplement

The Cryosphere Open Access EGU

Supplement of

Challenges in identifying Antarctic coastal polynyas in satellite observations and climate model output to support ecological climate change research

Laura L. Landrum et al.

Correspondence to: Laura L. Landrum (landrum@ucar.edu)

1 Supplemental material

The figures in this supplement provide further details for readers who are interested in seeing results for months, seasons (e.g. Figures S1-S2, S5-S6), regions (e.g. Figures S7) and/or example SIC and SIT thresholds not shown in the main manuscript. Supplemental Figure 2 shows integrated southern hemisphere (SH) sea ice area and sea ice extent for the NOAA and OSISAF CDRs. Also shown here are figures showing the impacts of degrading the CESM-JRA sea ice output to more closely resemble data based on passive microwave images (Figures S3-S4). Figures 3-5 show integrated SH polynya areas for each month of the year for the NOAA CDR (Figure S3), OSISAF CDR (Figure S4) and the JRA-CESM (Figure S5). Timeseries of integrated SH coastal polynya areas and numbers are shown for the annual average and four seasons for the CDRs and the JRA-CESM (Figure S6). The following five figures (Figures S7-S11) show temporal correlations and trends, by month and annually, for the five Antarctic sectors shown in Figure 1 in the main text. The final two figures (Figures S12-S13) show maps of impacts on SIC means and standard deviations (stds) by degrading JRA-CESM output and comparing with the NOAA-CDR for the fall (AMJ) and winter (JJA).

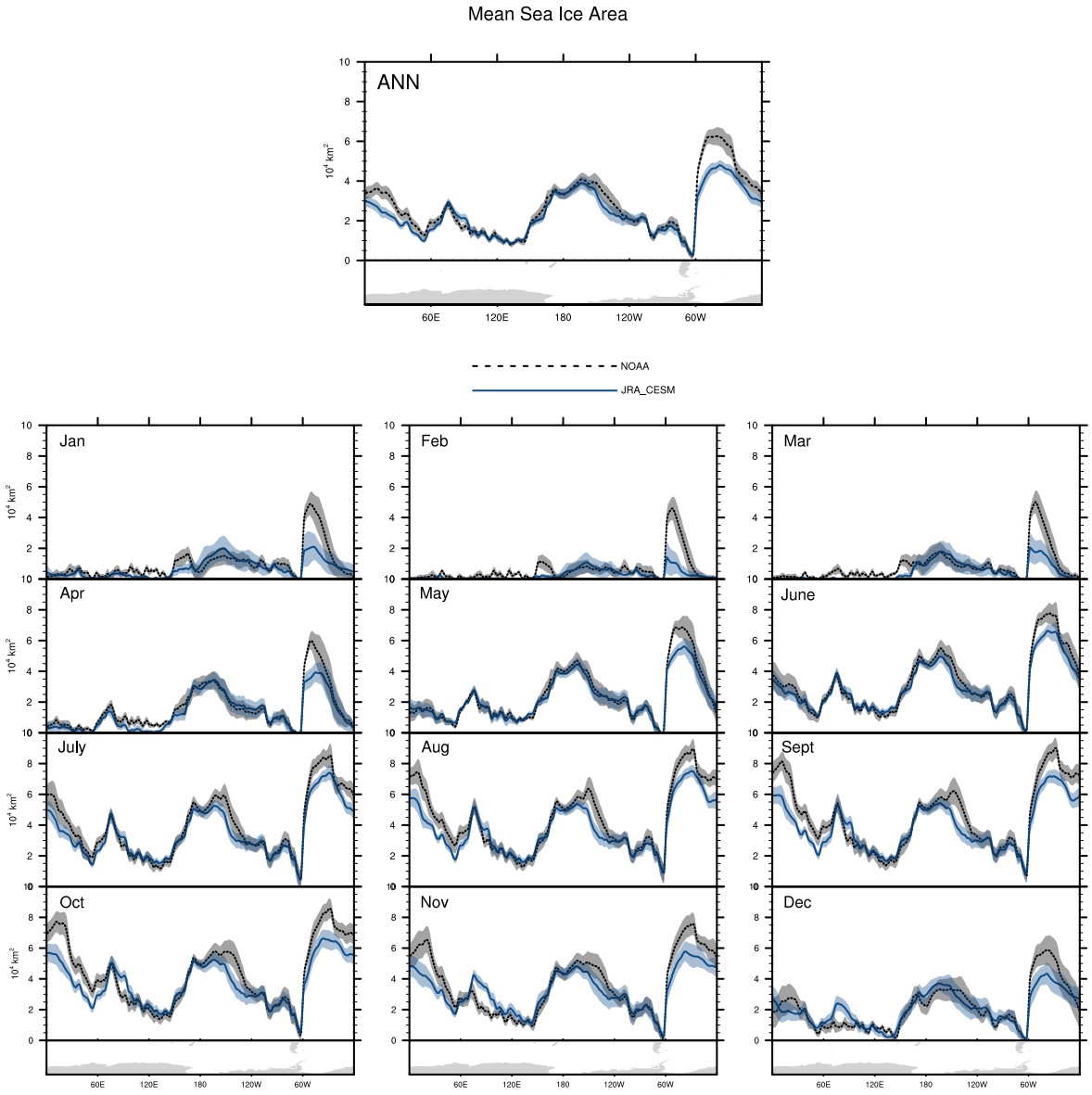

Figure S1. 1979-2020 Annual (top) and monthly (bottom panels) mean total sea ice extent as a function of longitude for the NOAA CDR (black) and the JRA-CESM (blue) data. Thick dashed (NOAA CDR) and solid lines (JRA-CESM) indicate the mean, shaded polygon indicates the mean ±1 standard deviation.

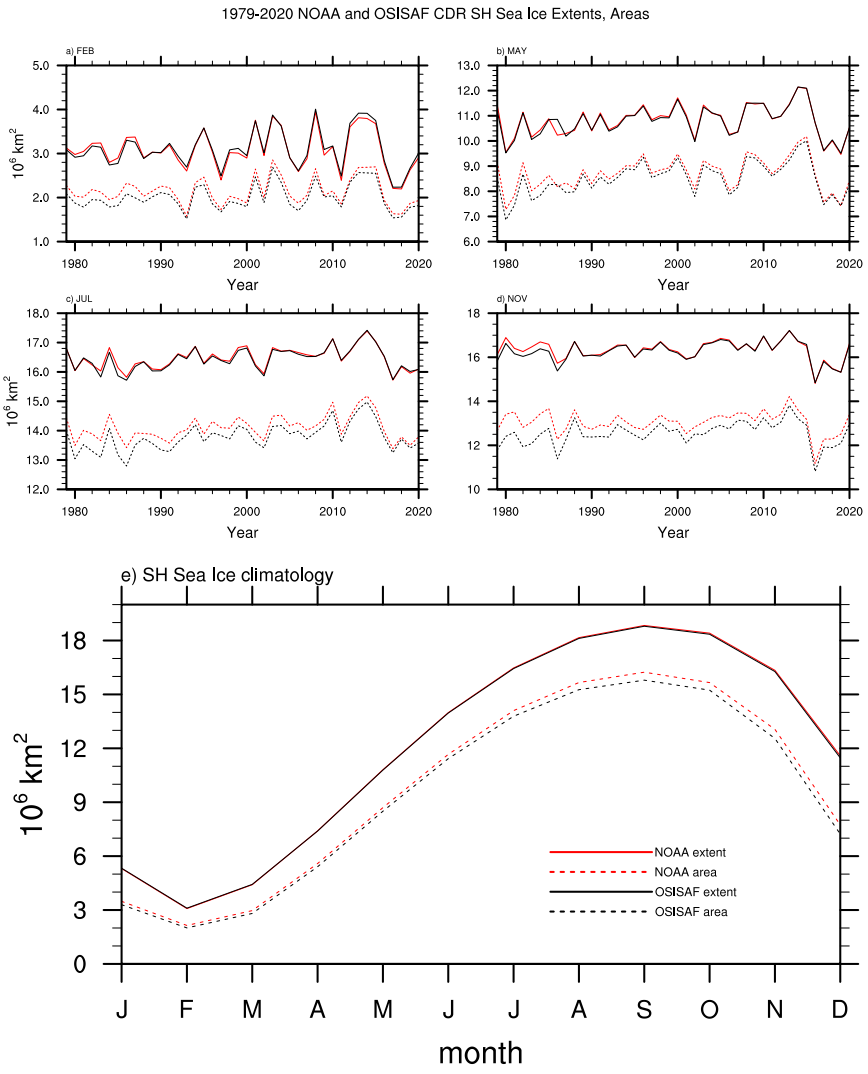

Figure S2. 1979-2020 integrated southern hemisphere (SH) sea ice extent (solid) and sea ice area (dashed) for the NOAA (red) and OSISAF (black) CDRs. Monthly timeseries are shown for a) February, b) May, c) July and d) November. Climatological monthly means are shown in e).

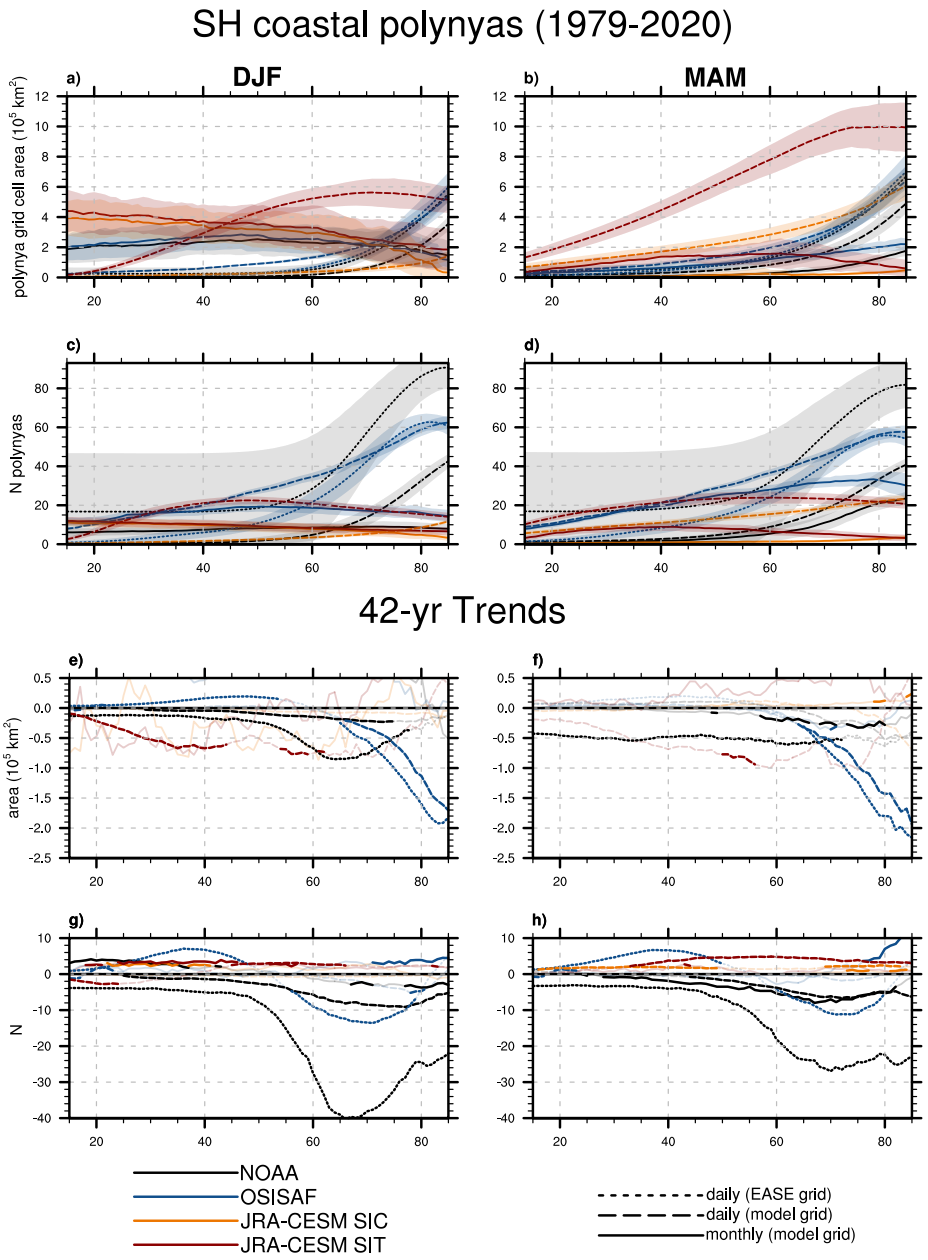

Figure S3. Total SH mean (1979-2020) coastal polynya areas (a-b), number of polynyas (c-d), 42-yr trends in polynya areas (e-f) and 42-yr trends in number of polynyas (g-h) as a function of threshold value (SIC, SIT) for summer (DJF; left column) and fall (MAM; right column) for NOAA (black), OSISAF (blue), and JRA-CESM (SIC metric, orange and SIT metric, maroon). Polynyas identified using the daily observational data on the original EASE grid are shown by dotted lines; dashed/solid lines indicate polynyas identified using daily/monthly data on the model grid. Climatological mean (1979-2020) values are shown in the thick lines; ±1 standard deviations shown by the lighter shading (a-d). Dark, thick dots/dashes/lines in the trends figures (e-h) indicate 95% or higher significance based on the Mann-Kendall non-parametric trend significance (Mann 1945; Kendall 1975; Gilbert 1987).

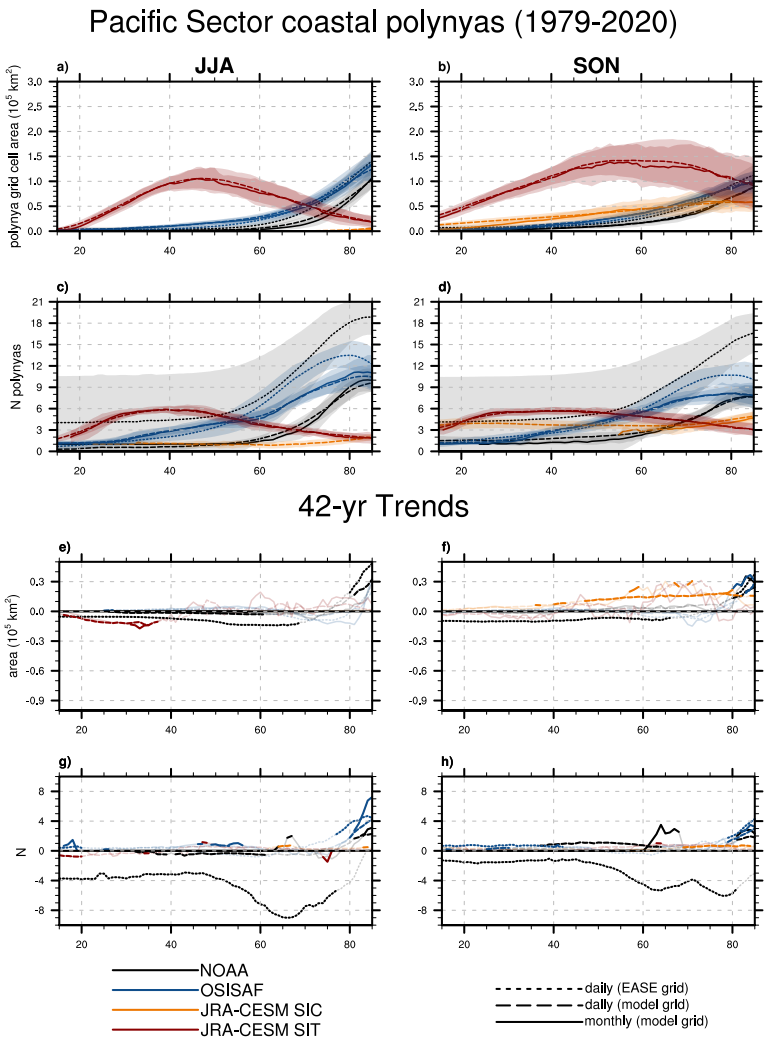

Figure S4. Same as Figure S3 except for winter (JJA) and spring (SON) seasons in the Pacific Sector.

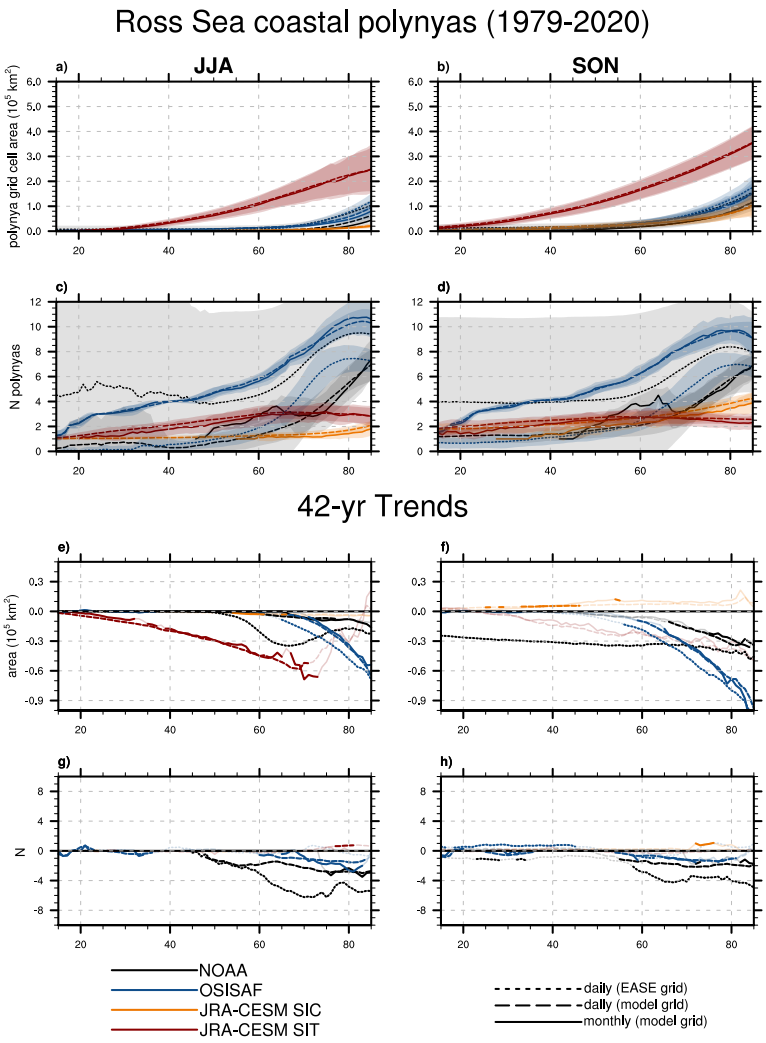

Figure S5. Same as Figure S4 for the Ross Sea.

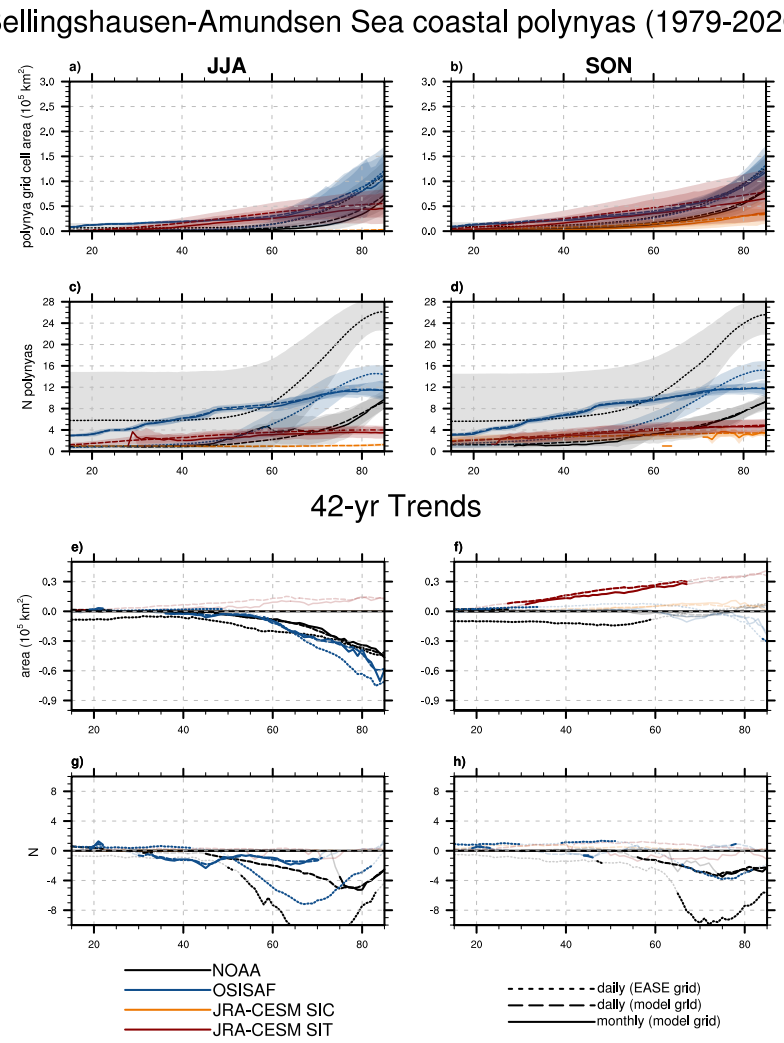

Figure S6. Same as Figure S4 for the Bellingshausen-Amundsen Sea.

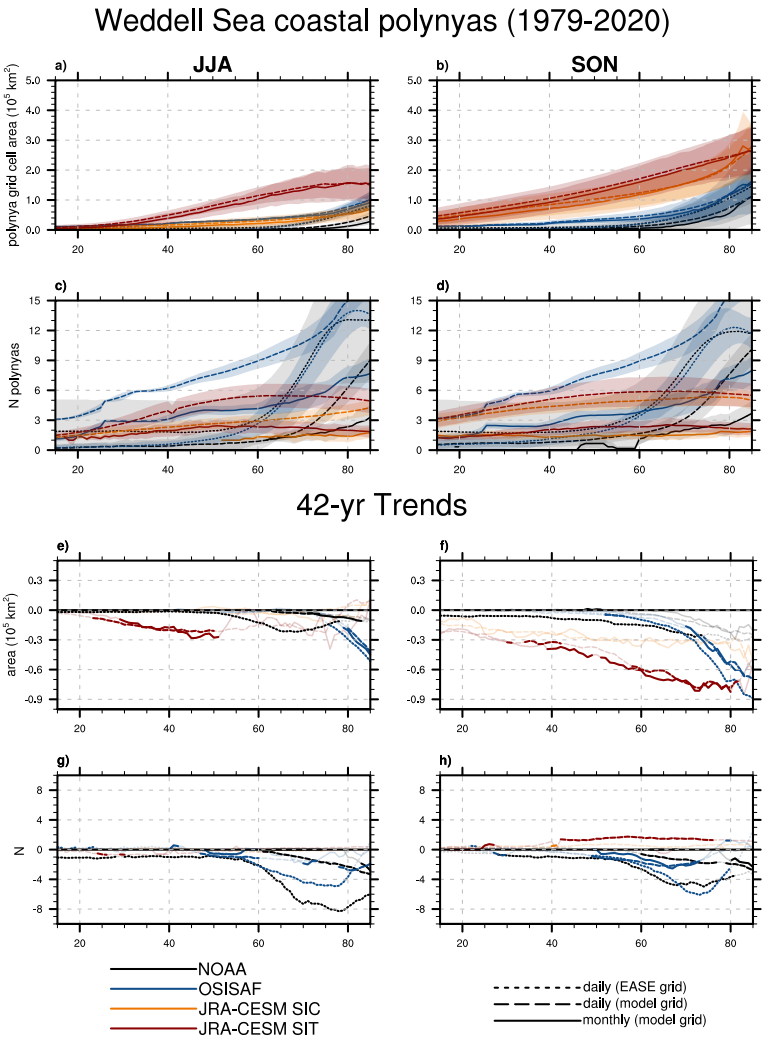

Figure S7. Same as Figure S4 for the Weddell Sea.

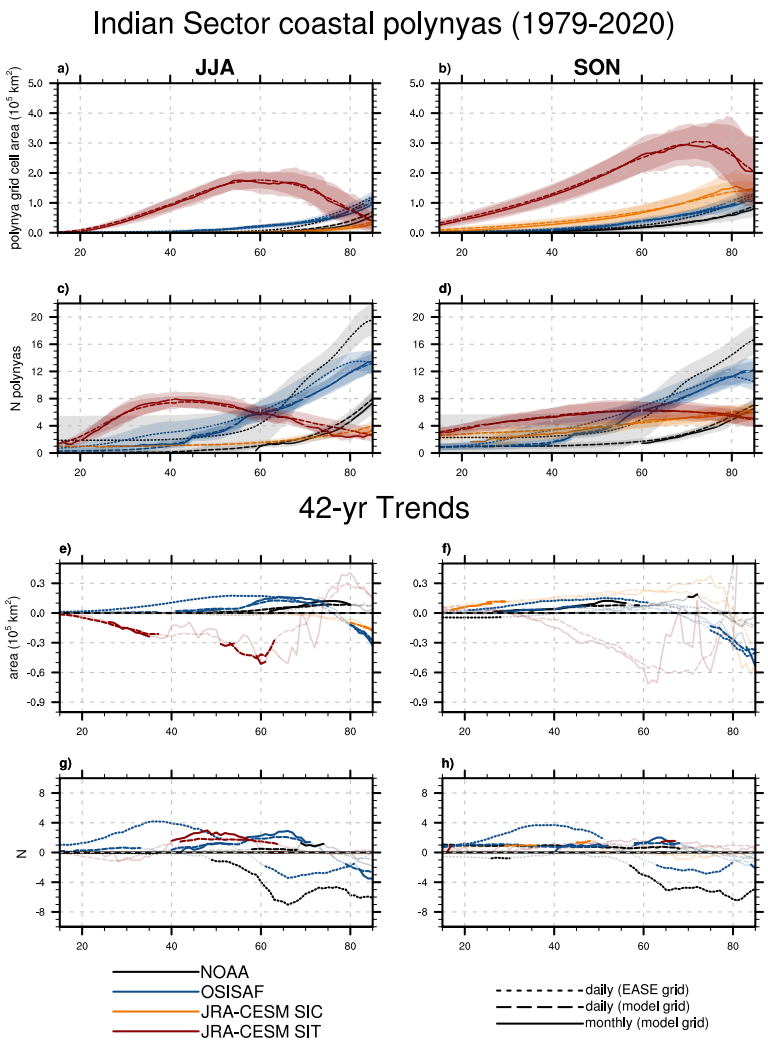

Figure S8. Same as Figure S4 for the Indian Sector.

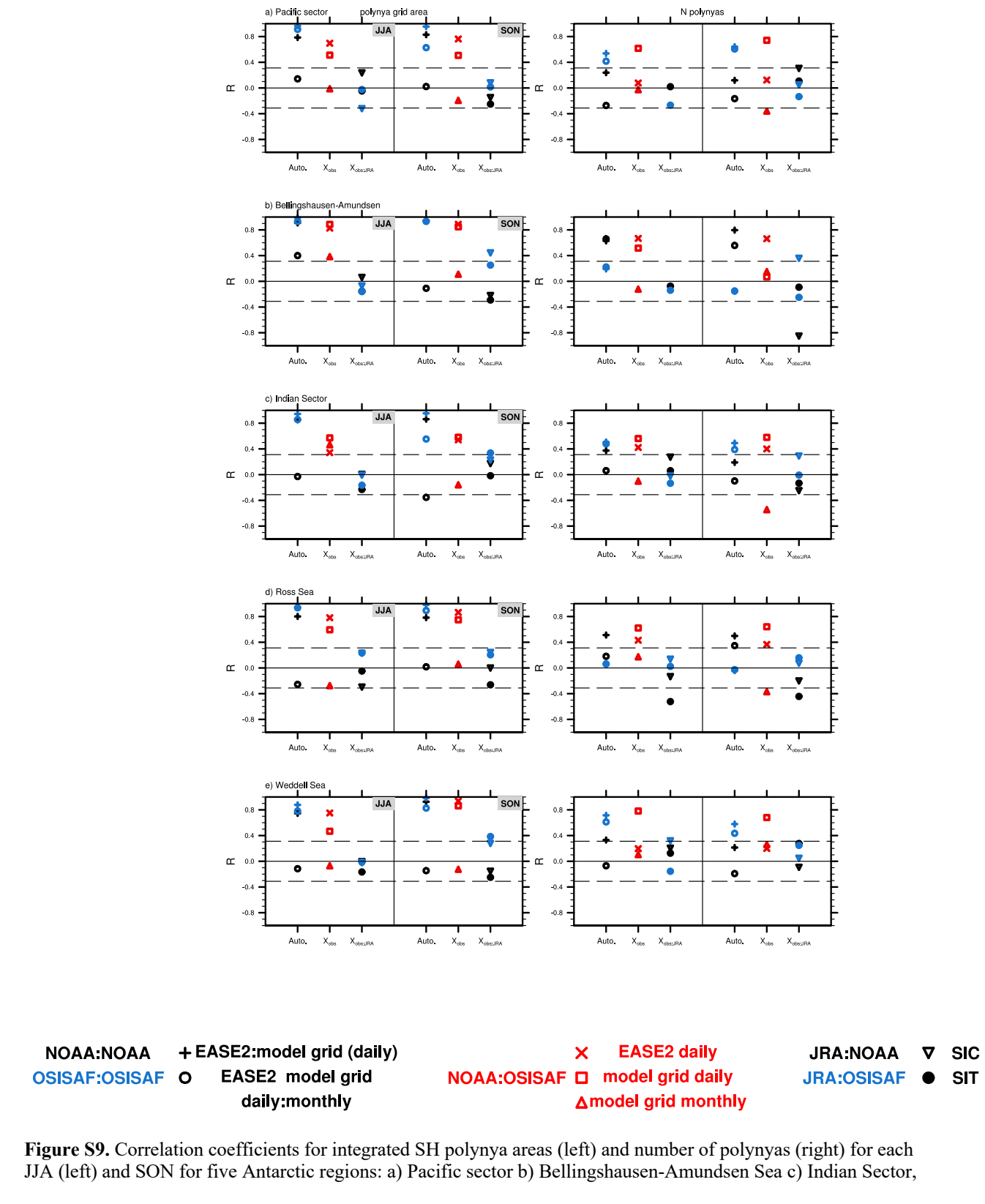

Figure S9. Correlation coefficients for integrated SH polynya areas (left) and number of polynyas (right) for each JJA (left) and SON for five Antarctic regions: a) Pacific sector b) Bellingshausen-Amundsen Sea c) Indian Sector,

d) Ross Sea and e) Weddell Sea. Autocorrelations are calculated between different grids ("regridding") for same observational product (NOAA black; OSISAF, blue); cross-correlations between the two observational products (NOAA:OSISAF, red) and between the observational products and the JRA-CESM (obs:JRA; NOAA black; OSISAF, blue). Symbols show correlations between time/longitude polynya time series from the daily observational data on the original EASE grid vs daily (+) and monthly (o) regridded on the model grid; NOAA:OSISAF on the EASE grid (x) and then regridded daily (□) and monthly (open triangles); and between JRA-CESM polynyas identified using SIT 0.4 m (•) and SIC 85% metric (inverted open triangles). Dashed horizontal lines in a-c indicate the 95% significance level based on the Mann-Kendall non-parametric trends significance (Mann 1945; Kendall 1975; and Gilbert 1987).

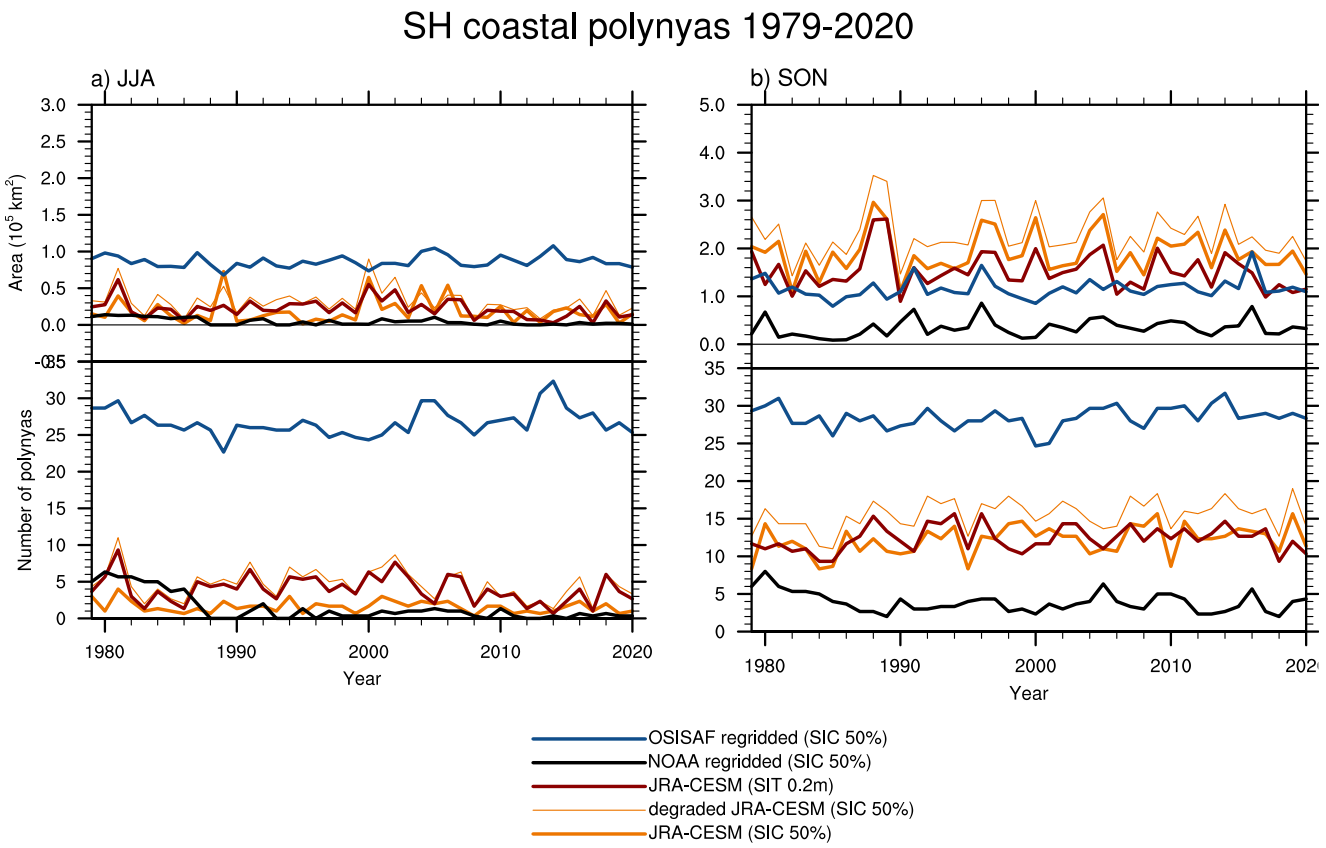

Figure S10. Southern Hemisphere (SH) 1979-2020 winter (JJA; a) and spring (SON; b) mean coastal polynya area (top panels) and number of individual polynyas (bottom panels). Polynya timeseries are for monthly NOAA (black) and OSISAF (blue) CDR data regridded onto the CESM grid, JRA-CESM model simulation using monthly SIC (orange) and SIT (brown), and the JRA-CESM model SIC degraded to more closely mimic satellite SICs (orange thin line). Thresholds are 50% for SIC and 0.2 m for SIT.

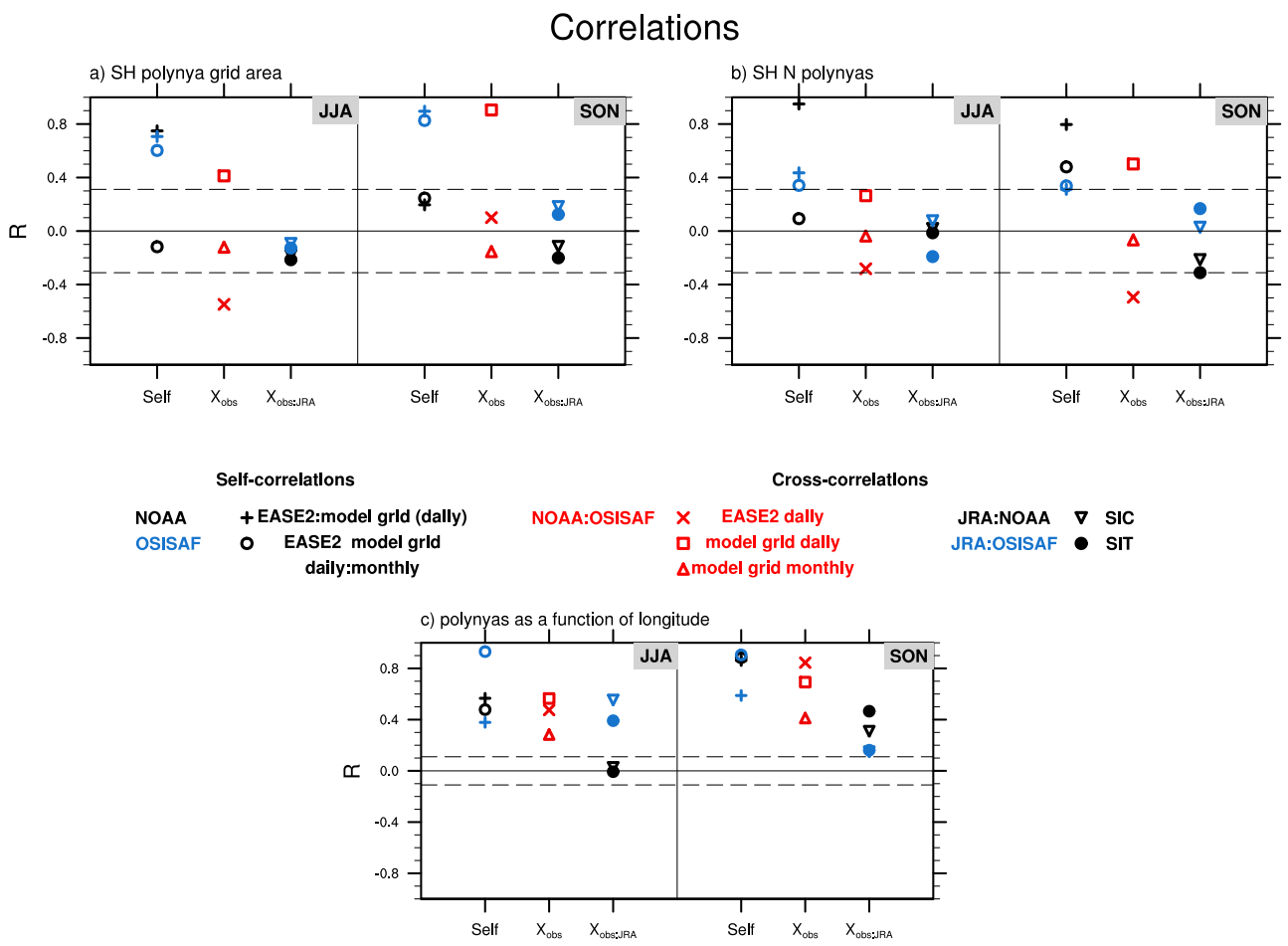

Figure S11. Correlation coefficients for integrated SH polynya areas (a), number of polynyas (b) and polynyas as a function of longitude (c) for each JJA (left) and SON (right). Self-correlations are calculated between different grids ("regridding") for same observational product (NOAA black; OSISAF, blue); cross-correlations between the two observational products (NOAA:OSISAF, red) and between the observational products and the JRA-CESM (obs:JRA; NOAA black; OSISAF, blue). Symbols show correlations between time/longitude polynya time series from the daily observational data on the original EASE grid vs daily (+) and monthly (o) regridded on the model grid; NOAA:OSISAF on the EASE grid (x) and then regridded daily (□) and monthly (open triangles); and between JRA-CESM polynyas identified using SIT 0.2 m (•) and SIC 50% metric (inverted open triangles). Dashed horizontal lines in a-c indicate the 95% significance level based on the Mann-Kendall non-parametric trends significance (Mann 1945; Kendall 1975; and Gilbert 1987).

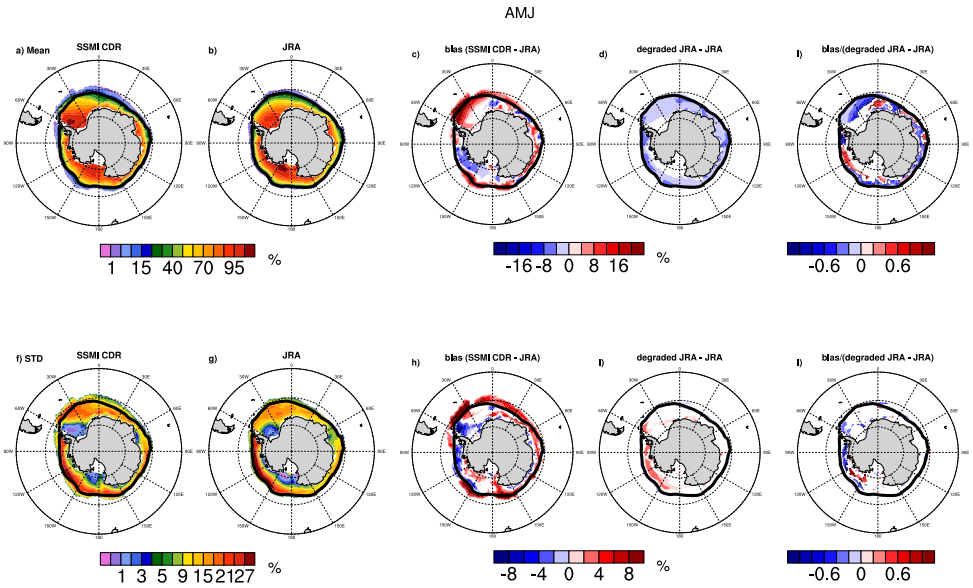

Figure S12. April-May-June (AMJ) climatological (1979-2020) SIC mean (top row) and standard deviation (bottom row) for NOAA-CDR (a, f), CESM JRA (b, g), NOAA-CDR-model bias (CDR-JRA, c, h), degraded JRA SIC - JRA SIC (d, i), and the satellite-model bias divided by the degraded-JRA model output (e, j). The 15% SIC contour from the CESM-JRA is shown by the heavy black contour in each of the maps. Differences less than ±1% have been masked out for visual clarity.

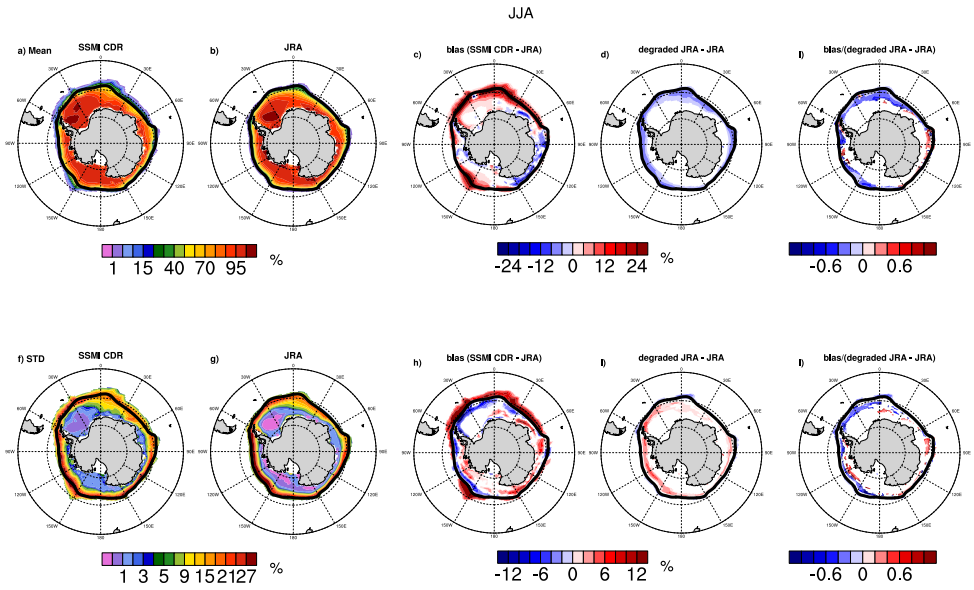

Figure S13. Same as Figure S12 except for June-July-August (JJA).